Available online at www.sciencedirect.com
ScienceDirect
Catalysis Today 132 (2008) 109–116
CATALYSIS TODAY
www.elsevier.com/locate/cattod

Kinetics of CO and H_2 oxidation over $CuO\text{-}CeO_2$ catalyst in H_2 mixtures with CO_2 and H_2O

Hyun Chan Lee, Dong Hyun Kim *

Department of Chemical Engineering, Kyungpook National University, 1370 Sankyukdong, Daegu 702-701, Republic of Korea

Available online 16 January 2008

Abstract

The kinetics of CO and H_2 oxidation over a $CuO\text{-}CeO_2$ catalyst were simultaneously investigated under reaction conditions of preferential CO oxidation (PROX) in hydrogen-rich mixtures with CO_2 and H_2O. An integral packed-bed tubular reactor was used to produce kinetic data for power-law kinetics for both CO and H_2 oxidations. The experimental results showed that the CO oxidation rate was essentially independent of H_2 and O_2 concentrations, while the H_2 oxidation rate was practically independent of CO and O_2 concentrations. In the CO oxidation, the reaction orders were 0.91, −0.37 and −0.62 with respect to the partial pressure of CO, CO_2 and H_2O, respectively. In the H_2 oxidation, the orders were 1.0, −0.48 and −0.69 with respect to the partial pressure of H_2, CO_2 and H_2O, respectively. The activation energies of the CO oxidation and the H_2 oxidation were 94.4 and 142 kJ/mol, respectively. The rate expressions of both oxidations were able to predict the performance of the PROX reactor with accuracy. The independence between the CO and the H_2 oxidation suggested different sites for CO and H_2 adsorption on the $CuO\text{-}CeO_2$ catalyst. Based on the results, we proposed a new reaction model for the preferential CO oxidation. The model assumes that CO adsorbs selectively on the Cu^+ sites; H_2 dissociates and adsorbs on the Cu^0 sites; the adsorbed species migrates to the interface between the copper components and the ceria support, and reacts there with the oxygen supplied by the ceria support; and the oxygen deficiency on the support is replenished by the oxygen in the reaction mixture.

Keywords: PROX; CO oxidation; H_2 oxidation; CO clean-up; $CuO\text{-}CeO_2$; Kinetics; Reaction model

1. Introduction

Hydrogen mixtures for proton exchange membrane fuel cells (PEMFCs) should be essentially free of CO as it poisons the anode catalyst of the fuel cell and considerably deteriorates the fuel cell performance. Typical hydrogen mixtures from reformers, however, contain 0.5–2% CO. The CO content can be lowered to less than 10 ppm by the preferential oxidation of CO (PROX), in which $CO + 1/2\ O_2 \rightarrow CO_2$ occurs preferentially over $H_2 + 1/2\ O_2 \rightarrow H_2O$. For an efficient PROX reaction, the catalyst used in the reaction should exhibit a high catalytic activity and a high selectivity for the CO oxidation in order to minimize consumption of the H_2 for fuel cells.

A number of catalysts have been proposed for the PROX reaction. Supported noble metal catalysts (Pt, Ru, Au, etc.) showed high activities and fair selectivities of 0.3–0.5 when the CO concentration of the hydrogen mixture was not very low [1–3]. A PROX reactor model for a reactor with a noble metal catalyst has, however, shown that it is very difficult to remove CO to less than tens of ppm in a single reactor due to extremely poor selectivity of the catalyst at very low CO concentrations [4]. Hence a staged reactor was used for the CO clean-up with Pt catalysts [5,6]. On the other hand, ceria supported copper catalysts were found to have high catalytic activity, comparable or better than the noble metal catalysts, and excellent selectivity [7–13]. Indeed, an isothermal reactor packed with a $CuO\text{-}CeO_2$ catalyst has been demonstrated to remove CO from 10,000 ppm to less than 10 ppm [10]. In view of the remarkable performance and the high price of noble metals, the base metal catalyst, $CuO\text{-}CeO_2$, is considered as an economical, attractive catalyst for the PROX reaction.

In view of many papers on the PROX reaction over $CuO\text{-}CeO_2$, there have been only a few that addressed CO oxidation kinetics for the catalyst. Liu and Flytzani-Stephanopolous [14] proposed a rate expression for CO oxidation over $CuO\text{-}CeO_2$ catalysts. Sedmark et al. [15] proposed a Mars and van

* Corresponding author. Tel.: +82 53 950 5617; fax: +82 53 950 6615.
E-mail address: dhkim@knu.ac.kr (D.H. Kim).

0920-5861/$ – see front matter © 2007 Elsevier B.V. All rights reserved.
doi:10.1016/j.cattod.2007.12.028

Krevelen type expression for the CO oxidation in excess hydrogen. Later, Sedmark et al. [16] also proposed a transient kinetic model of CO oxidation based on a detailed kinetic model and transient experiments. Although CuO-CeO_2 catalysts show high selectivity toward CO oxidation, hydrogen oxidation simultaneously occurs and its rate can be considerably fast at high temperatures. To minimize the hydrogen oxidation and at the same time to remove CO to a desired level, usually around 10 ppm, information on the CO oxidation as well as the H_2 oxidation is necessary, but the previous kinetic studies have considered only the CO oxidation.

Moreover, the H_2-rich reformer effluents from fuel processors contain considerable amounts of CO_2 and H_2O, and the performance of CuO-CeO_2 has been reported to be adversely affected by the presence of CO_2 and H_2O in the reaction mixtures. For reaction mixtures with CO_2 and H_2O, the reaction temperature had to be increased around 30–50 °C to obtain a similar CO conversion observed in the absence of the two components [9,11]. To be useful, the PROX kinetics should be able to account for the effect of CO_2 and H_2O on the oxidation rate of CO and H_2.

With this in context, the present study aims to provide kinetics of CO oxidation and H_2 oxidation in the presence of CO_2 and H_2O in the reaction mixture. In this respect, this kinetic study is the first that considers CO oxidation simultaneously with H_2 oxidation in hydrogen mixtures with CO_2 and H_2O.

2. Experimental

2.1. Catalyst

The CuO-CeO_2 catalyst was prepared by the method of coprecipitation. Under vigorous stirring, a NaOH solution (1N) was added to a solution of Cu and Ce nitrates at 70 °C and the pH of the solution was controlled at 10. The precipitate was aged for 5 h at the same condition. It was filtered, washed with deionized water and dried in an oven at 90 °C for 12 h. The dried sample was calcined at 500 °C for 5 h in air. The Cu content was 20 at% (=Cu/(Cu + Ce) × 100) and the specific surface area measured by the nitrogen adsorption was 119 m^2/g.

2.2. Kinetic experiment

The reactor was made of 6.25 mm (OD) stainless steel tube. In the reactor, 50 mg of the catalyst of 150–180 μm in size was diluted with 950 mg of glass beads of the same size to facilitate dissipation of the reaction heat. A thermocouple was inserted into the middle of the catalyst bed to monitor the reaction temperature. The reactor temperature was varied in the range 100–240 °C. Before the reaction, the catalyst was reduced under H_2 at 300 °C. The feed flow rate was 100 ml (STP)/min and a typical feed composition was 1% CO, 1% O_2, 50% H_2, 16% CO_2, 16% H_2O and 16% He (inert). In the kinetic experiments, however, CO in the feed was varied between 0.5 and 4%, O_2 in the range of 0.5–4%, CO_2 in the range of 4–16%, H_2O in the range of 4–20%, and H_2 in the range of 10–50%. A water bubbler was used to feed the water vapor, and the vapor content was controlled by the temperature of the bubbler. After the reactor, a water trap at 0.2 °C was used to remove the water vapor in the effluent stream. The composition of the reactor effluent was analyzed on line with a gas chromatography (HP 5890A). A Caboxen column (Supelco) was used to separate O_2, CO and CO_2. By comparing the GC peak area of CO (A_{CO}) with the area at zero conversion (A_{CO} at $X_{CO} = 0$), obtained before the experiment, the CO conversion was calculated. The O_2 conversion (X_{O_2}) was determined similarly by comparing the peak areas.

$$X_{CO} = 1 - \frac{A_{CO}}{A_{CO}\,\text{at}\,X_{CO}=0}, \quad X_{O_2} = 1 - \frac{A_{O_2}}{A_{O_2}\,\text{at}\,X_{O_2}=0} \tag{1}$$

The selectivity for CO oxidation (S) was determined by

$$S = \frac{F_{CO}X_{CO}}{2F_{O_2}X_{O_2}} \tag{2}$$

where F_{CO} and F_{O_2} are the molar flow rate of CO and O_2 in the feed, respectively.

3. Results

3.1. CO oxidation in the presence or absence of H_2

Fig. 1 compares the CO conversion obtained in the presence or absence of 50% H_2 in the feed. Without H_2 in the feed the only reaction occurs in the reactor is pure CO oxidation. In this case the selectivity of CO oxidation, S, is always 100% and the oxygen conversion is at most 50%. Fig. 1 shows that the presence of 50% H_2 in the feed did not affect the CO conversion up to the reaction temperature of around 200 °C, where the CO conversion was 98%. But the selectivity S was 100% until around 150 °C and decreased with increasing temperature. This indicates that H_2 oxidation occurred above 150 °C and its rate increased with temperature, consuming an increasing portion of the input oxygen and hence decreasing the selectivity. In the

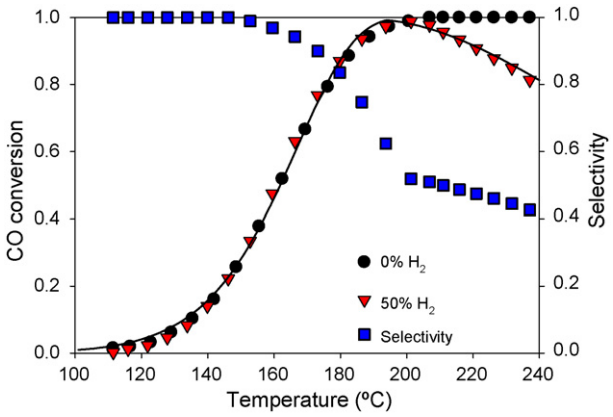

Fig. 1. CO conversion in the presence and absence of H_2 in the feed. Symbols are experimental data and line is calculated CO conversion. Feed: 100 ml/min, 1% CO, 1% O_2, H_2 (shown), 16% CO_2, 16% H_2O, balance He. Catalyst: 50 mg CuO-CeO_2.

presence of H_2, the complete conversion of oxygen coincided with the CO conversion maximum around 200 °C, and above 200 °C, the oxygen was depleted inside the reactor by the two oxidation reactions.

The reverse water gas shift reaction ($CO_2 + H_2 \rightarrow CO + H_2O$) may occur in the part of the PROX reactor where oxygen is depleted. To examine whether the reverse water gas shift reaction caused the decrease in the observed CO conversion above 200 °C, we carried out an experiment in which the feed was consisted of 16% CO_2, 50% H_2 and balanced with He. We found the catalyst was quite inactive for the reverse water gas shift reaction and observed only a trace amount of CO around 200 ppm at 250 °C. Similar results have also been reported by Marino et al. [12]. The decrease in the CO conversion above 200 °C was solely due to the hydrogen oxidation, the rate of which increased much faster than the CO oxidation rate with increasing temperature. The H_2 oxidation and the CO oxidation competed for oxygen, and the H_2 oxidation consumed an increasing portion of the input oxygen with temperature in the reactor. This indicates that the activation energy of H_2 oxidation is larger than that of the CO oxidation. In the temperature range 150–200 °C, where oxygen was available throughout the reactor, the CO oxidation was independent of the H_2 oxidation and the H_2 partial pressure.

3.2. Effect of concentrations of O_2, CO, CO_2 and H_2O on PROX

Fig. 2 shows the effect of O_2 concentration in the feed on the CO conversion. When oxygen was available throughout the reactor, the observed CO conversion was virtually independent of the oxygen concentrations. The maximum CO conversion, however, was dependent on the input oxygen concentration. For the feed of 0.5% O_2, the maximum CO conversion was 76% because of the concomitant hydrogen oxidation, and for the feed of 1% or higher oxygen concentrations, a near complete or complete CO conversion was possible. In this case, the temperature window for complete CO removal extended with increasing oxygen feed concentration. It is well known that ceria has high oxygen storage capacity and can acts as oxygen buffer [17]. If the oxygen concentration in the reaction mixture is greater than the minimum oxygen concentration for saturation of the oxygen storage capacity, the oxygen concentration on the surface would be nearly constant, and hence the CO oxidation rate would be independent of the oxygen concentration. As the oxygen concentration tends to zero, a relation between the reaction rate and the oxygen concentration would eventually appear, but as it turns out such a dependency at low oxygen concentration has had little effect on the observed exit CO conversion of the PROX reactor. This indicates that for typical PROX operations, the reaction rate can be presented as a zero-order reaction with respect to the oxygen concentration. Indeed, reaction orders close to zero have been reported for the oxygen partial pressure [14,15].

Fig. 3 shows the effect of CO concentration on the CO conversion. Since the oxygen concentration in the feed was fixed at 1%, the maximum CO conversion depended on the input CO concentration. For the feed with 2% CO, for example, the maximum CO conversion would be 100% if all the input oxygen was consumed by the CO oxidation. As H_2 oxidation also consumed the oxygen, the maximum CO conversion in the presence of 50% H_2 was always less than the maximum CO conversion for CO oxidation alone. At temperatures above the temperature corresponding to the maximum CO conversion, the oxygen was depleted in the reactor and became the limiting reactant. In the temperature ranges where oxygen was not the limiting reactant in the reactor, the CO conversions for the various feed CO concentrations in the range of 0.5–4% were similar but slightly decreased with increasing feed CO concentration, indicating that the amount of CO converted to CO_2 was roughly proportional to the CO concentration.

The effect of CO_2 concentration on the CO conversion is shown in Fig. 4. The CO conversion decreased with increasing

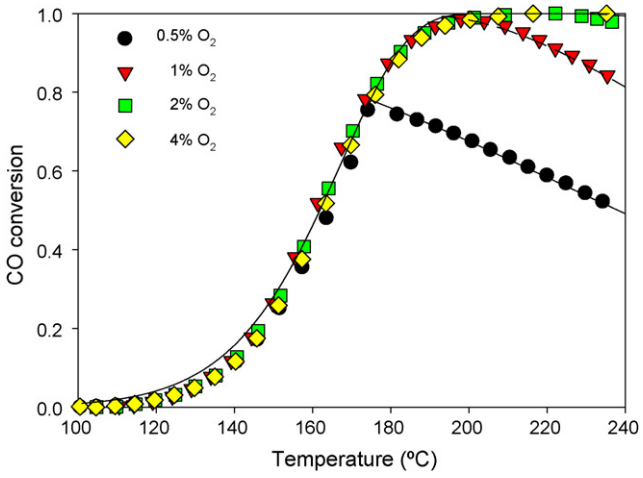

Fig. 2. Effect of feed O_2 concentration on CO conversion. Symbols are experimental conversion and lines are calculated conversion. Feed: 100 ml/min, 1% CO, O_2 (shown), 50% H_2, 16% CO_2, 16% H_2O, balance He. Catalyst: 50 mg CuO-CeO_2.

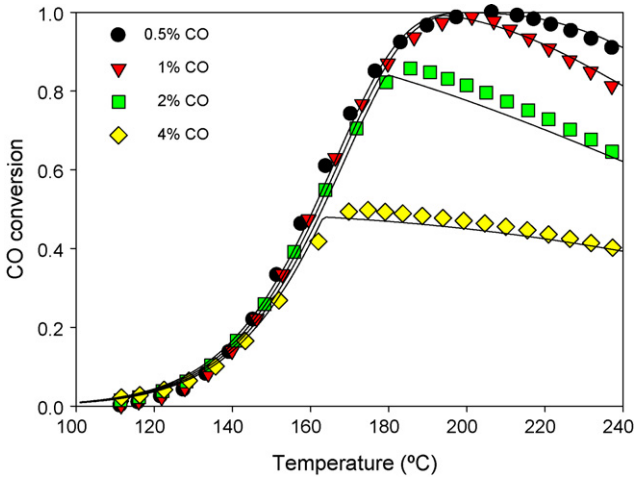

Fig. 3. Effect of CO concentration on CO conversion. Symbols are experimental conversion and lines are calculated conversion. Feed: 100 ml/min, CO (shown), 1% O_2, 50% H_2, 16% CO_2, 16% H_2O, balance He. Catalyst: 50 mg CuO-CeO_2.

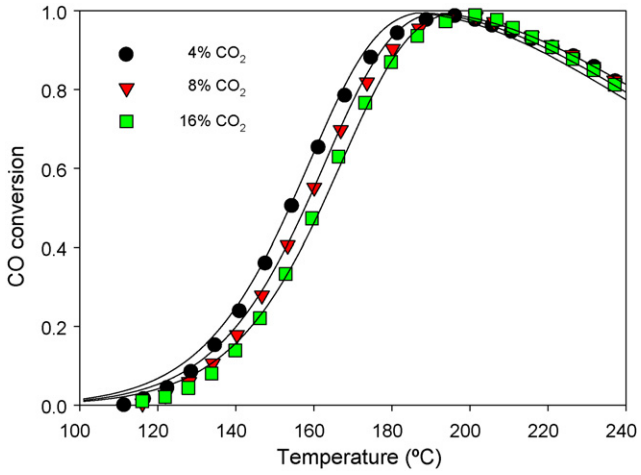

Fig. 4. Effect of CO_2 concentration on CO conversion. Symbols are experimental conversion and lines are calculated conversion. Feed: 100 ml/min, 1% CO, 1% O_2, 50% H_2, CO_2 (shown), 16% H_2O, balance He. Catalyst: 50 mg CuO-CeO_2.

CO_2 concentration in the feed, showing an inhibition effect of CO_2 on the CO oxidation, in agreement with previous studies [9–11]. Fig. 5 shows the effect of H_2O concentration on the CO conversion. The CO conversion significantly decreased with increasing H_2O concentration.

Since the CO oxidation rate is independent of H_2 and O_2 partial pressures, a rate expression for the CO oxidation in a power-law form can be given as

$$-r_{CO} = k_{CO} P_{CO}^{a} P_{CO_2}^{b} P_{H_2O}^{c} \quad \text{where}$$
$$k_{CO} = A_{CO} \exp\left(\frac{-E_{CO}}{RT}\right) \tag{3}$$

The reaction order a would be close to one, as the rate is roughly proportional to the CO partial pressure, and the orders b and c would be negative numbers, because both CO_2 and H_2O inhibits the oxidation.

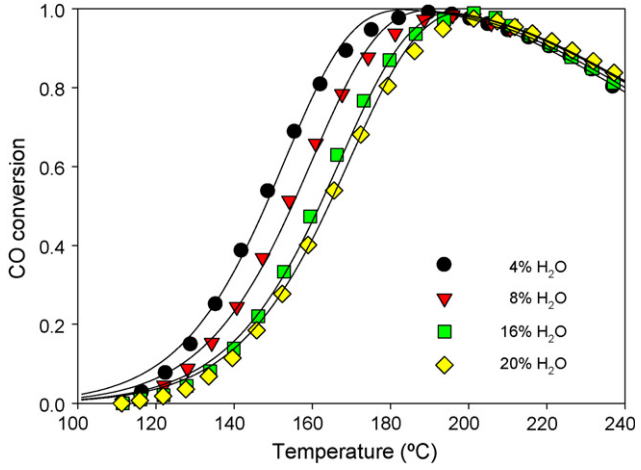

Fig. 5. Effect of H_2O concentration on CO conversion. Symbols are experimental conversion and lines are calculated conversion. Feed: 100 ml/min, 1% CO, 1% O_2, 50% H_2, 16% CO_2, H_2O (shown), balance He. Catalyst: 50 mg CuO-CeO_2.

3.3. Hydrogen oxidation

In the PROX, hydrogen oxidation also occurs and consumes oxygen, which otherwise can be used for CO oxidation. Suppressing the hydrogen oxidation is important to have high selectivity in the PROX. In Fig. 1, it is shown that the selectivity of CO oxidation was 100% at low temperatures below 150 °C. The selectivity decreased with temperature and was around 50% at 200 °C, where the input oxygen was completely consumed in the reactor. The amount of oxygen consumed by hydrogen oxidation can be determined by deducting the amount consumed by CO oxidation from the total amount of consumed oxygen, i.e. $F_{O_2}X_{O_2} - (1/2)F_{CO}X_{CO} (= F_{O_2}X_{O_2}(1-S))$. Fig. 6 shows the O_2 conversion by H_2 oxidation $(= X_{O_2}(1-S))$ in the reactor for the feed compositions of different CO content. In the absence of CO, the O_2 conversion by H_2 oxidation gradually increased to 1.0 around 220 °C. For the feed with 1% CO, the O_2 conversion followed the conversion line of pure H_2 oxidation until around 200 °C and then deviated from the line at temperatures above 200 C. While oxygen was not depleted in the reactor, the O_2 conversion by H_2 oxidation was independent of CO concentrations in the range of 0–1%. Fig. 7 shows the effect of O_2 concentration on the H_2 oxidation. The amount of O_2 consumed by the H_2 oxidation was little affected by the feed O_2 concentration, indicating that the H_2 oxidation rate was practically independent of O_2 concentration, similar to the CO oxidation. In addition, it was observed that the H_2 oxidation rate is proportional to the H_2 partial pressure (not shown), leading to a first-order rate expression with respect to the H_2 partial pressure.

Bae et al. [11] recently investigated the effect of CO_2 and H_2O in the feed on the H_2 oxidation activity over a similar CuO-CeO_2 catalyst. They reported that the addition of CO_2 or H_2O to the feed considerably decreased the H_2 oxidation activity and increased the reaction temperature by 15–30 °C to get the same O_2 conversion by H_2 oxidation observed in the absence of CO_2 and H_2O.

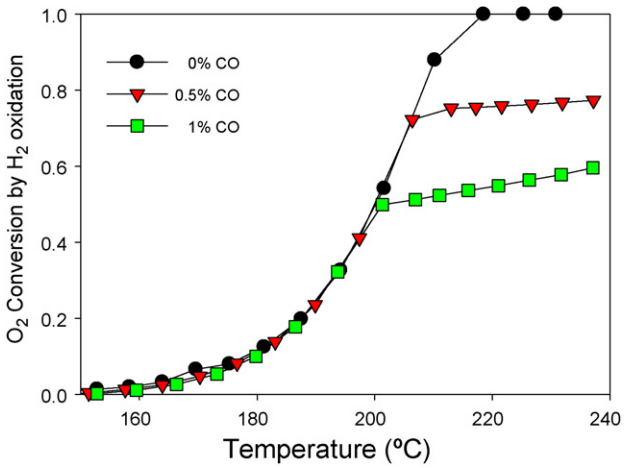

Fig. 6. Effect of CO concentration on O_2 conversion by H_2 oxidation. Feed: 100 ml/min, CO (shown), 1% O_2, 50% H_2, 16% CO_2, 16% H_2O, balance He. Catalyst: 50 mg CuO-CeO_2.

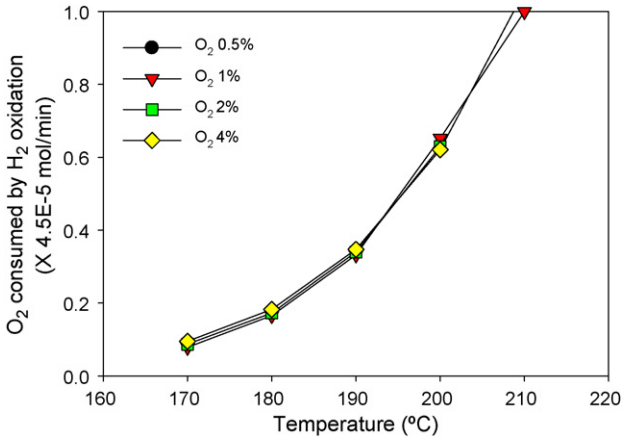

Fig. 7. Effect of feed O2 concentration on the amount of O2 consumed by H2 oxidation. Feed: 100 ml/min, O2 (shown), 50% H2, 16% CO2, 16% H2O, balance He. Catalyst: 50 mg CuO-CeO_2.

Based on the results of this study and those in literature, the kinetic expression for H_2 oxidation in the PROX is assumed as

$$-r_{H_2} = k_{H_2} P_{H_2} P_{CO_2}^{\alpha} P_{H_2O}^{\beta} \quad \text{where} \quad k_{H_2} = A_{H_2} \exp\left(\frac{-E_{H_2}}{RT}\right) \tag{4}$$

The exponents α and β would be negative numbers to account for the inhibition effect of CO_2 and H_2O on the H_2 oxidation.

3.4. Rate expressions of CO oxidation and H_2 oxidation

The experimental CO conversion varied from a few percent to 100%. When the conversion exceeds 10%, the concentration change along the reactor should be considered in the analysis of the experimental data. This approach is called the integral method as opposed to the differential method, where the conversion is kept small so that an average composition of the reactor can be used in the data analysis.

The reactor used in this study can be modeled as a plug-flow packed-bed reactor. The mass balance for CO is

$$F_{CO} \frac{dX_{CO}}{dW} = -r_{CO} \tag{5}$$

We consider O_2 mass balance instead of H_2 mass balance since O_2 is often a limiting reactant in the reaction. The balance for O_2 is

$$F_{O_2} \frac{dX_{O_2}}{dW} = -\frac{1}{2}(r_{CO} + r_{H_2}) \tag{6}$$

where F_{CO} is the molar feed rate of CO (mol/s); F_{O_2}, the molar feed rate of O_2; W, the catalyst weight variable (kg), running from 0 to W_t (the total weight of the catalyst in the reactor, 50 mg). The balance equations are integrated from $W = 0$ to $W = W_t$ with the initial condition (the condition at the reactor inlet):

$$X_{CO} = 0, \quad X_{O_2} = 0 \quad \text{at} \quad W = 0 \tag{7}$$

For a given composition and temperature, r_{CO} and r_{O_2} depend on the values of the kinetic parameters: A_{CO}, E_{CO}, a, b and c for CO oxidation; A_{H_2}, E_{H_2}, α and β for H_2 oxidation. The exit conversions of CO and O_2, calculated by simultaneous integration of Eq. (5) and Eq. (6) from $W = 0$ to $W = W_t$, become functions of the set of the parameters.

We fitted the calculated exit conversion to the experimental conversion by adjusting the parameters. It is not an easy task to determine all the nine parameters simultaneously by the fitting, if initial estimates of the parameters, which are close to the correct values, are not given. As the CO oxidation was independent of the H_2 oxidation, we first estimated the five kinetic parameters in the CO oxidation rate using the CO conversion data obtained at the conditions where the oxygen conversion was less than 1.0. We then estimated the remaining four parameters in the H_2 oxidation rate with the already estimated five parameters for the CO oxidation. To find the best fit, we defined an objective function Z:

$$Z = \sum_{i=1}^{i=N} (X_{CO,i}^{exp} - X_{CO,i}^{cal})^2 \tag{8}$$

where $X_{CO,i}^{exp}$ is the i-th experimental CO conversion, $X_{CO,i}^{cal}$ is the calculated CO conversion for the reaction condition of the i-th data, and N is the total number of conversion data. We searched for the minimum of Z by using the Nelder and Mead method developed for the minimization of a multivariable, unconstrained, nonlinear function [18]. Thus estimated rate expressions are

$$-r_{CO} = 3.4 \times 10^{10} \exp\left(\frac{-94.4\,\text{kJ/mol}}{RT}\right) \times P_{CO}^{0.91} P_{CO_2}^{-0.37} P_{H_2O}^{-0.62}\ \text{mol/kg/s} \tag{9}$$

$$-r_{H_2} = 6.1 \times 10^{13} \exp\left(\frac{-142\,\text{kJ/mol}}{RT}\right) \times P_{H_2} P_{CO_2}^{-0.48} P_{H_2O}^{-0.69}\ \text{mol/kg/s} \tag{10}$$

The partial pressures are in the unit of kPa. The lines in Figs. 1–5 are the calculated conversion with the rate expressions. Fig. 8

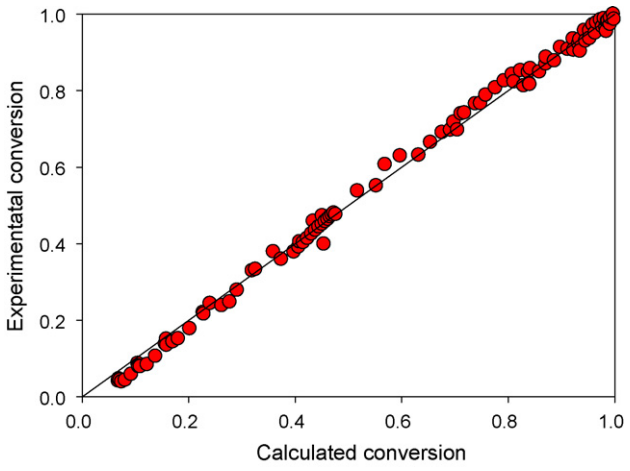

Fig. 8. Parity plot of CO conversions.

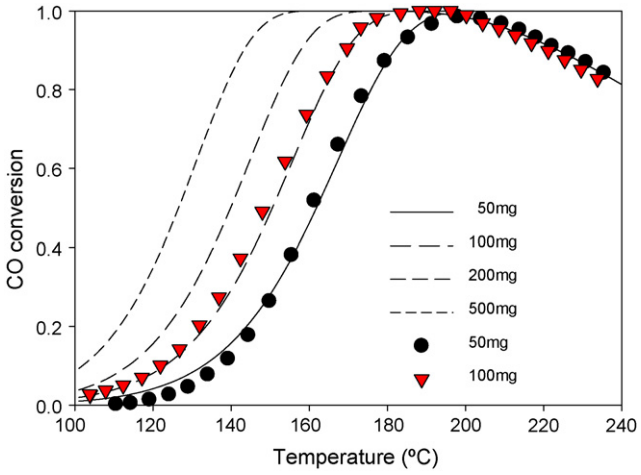

Fig. 9. Effect of catalyst weight on CO conversion. Symbols are experimental conversion and lines are calculated conversion. Feed: 100 ml/min, 1% CO, 1% O_2, 50% H_2, 16% CO_2, 16% H_2O, balance He.

compares the calculated exit CO conversion and the experimental CO conversion data employed in the fitting. The good agreement between the two conversions shows the validity of the rate expressions.

Finally, we compared the prediction of the rate expressions and the experimental data not used in the fitting. All the experimental data used in the fitting were obtained with a reactor packed with a 50 mg of the catalyst sample. We prepared another packed-bed reactor with a catalyst loading of 100 mg for the comparison. The results are shown in Fig. 9. The predictions are in excellent agreement with the experimental data, again demonstrating the validity of the rate expressions. It is also seen in the figure that increasing the catalyst loading or equivalently decreasing the space velocity extends the temperature window for complete removal of CO from the hydrogen mixture.

4. Discussion

4.1. Active sites of CO oxidation and H_2 oxidation

If the CO and H_2 oxidation reactions competed for a same active site, the oxidation rates of CO and H_2 must have been affected by the H_2 concentration and the CO concentration, respectively. The experimental data of this study attest that the CO oxidation and the H_2 oxidation over the CuO-CeO_2 catalyst are independent with each other. This suggests that the active site for the CO oxidation is different from that of the H_2 oxidation.

For the CO oxidation, a synergistic effect has been shown to exist between CeO_2 and Cu species in the CuO-CeO_2 catalyst [9,10,14,19–22]. The reaction has been shown to take place at the interface between the finely dispersed Cu particles and ceria, and small copper particles in close contact with the ceria support has been shown to be responsible for the catalytic activity [12,14–16,19,23]. The oxygen from the ceria support oxidizes the CO adsorbed on the Cu particles [14–16,19]. The H_2 oxidation is also thought to proceed similarly, adsorption of hydrogen on Cu particles and subsequent oxidation of the adsorbed hydrogen species by the oxygen supplied by the ceria support.

There are three oxidation states for Cu in the catalyst: Cu^0, Cu^+ and Cu^{2+}. It is well known that CO is easily desorbed from Cu^0 and Cu^{2+}, but it chemisorbs on Cu^+ sites [22,24]. Among the three copper species, only a Cu^+-carbonyl species was observed on a CuO-CeO_2 catalyst when it was exposed to a mixture of CO, H_2 and O_2 or a mixture of CO and O_2 [25–27]. A recent study reported that for a fully oxidized CuO-CeO_2 catalyst, around 70% of Cu^{2+} was reduced to Cu^+ by 1 Torr CO even at 300 K and the Cu^+ state remain unchanged under 1 Torr O_2 at 373 K [23,26,27], indicating a stabilized Cu^+ valance state on the catalyst. Interestingly Cu^+ has been shown to stably exist as the dominant copper species in CuO-CeO_2 even after reduction with hydrogen at 773 K [22]. As these results suggest, among the different oxidation states of the copper, it is far likely that Cu^+ is the site for CO adsorption during the PROX reaction, serving as the active site for the CO oxidation. This was proposed by Liu and Flytzani-Stephanopolous [14].

Based on the premise that the CO and H_2 oxidation reactions do not share the same active site, assigning Cu^+ to the site for CO adsorption leaves Cu^0 and Cu^{2+} as a possible hydrogen adsorption site. Hydrogen is known to selectively adsorb on metal phases. Hydrogen chemisorption has been used for measurement of metallic surface area of catalyst. Among various copper species, hydrogen was selectively adsorbed on the metallic copper [28]. The same would hold on the CuO-CeO_2, and we propose Cu^0 as the sites for hydrogen adsorption in the PROX reaction.

4.2. Reaction mechanism of the PROX reaction over the CuO-CeO_2

A redox mechanism was proposed by Martinez-Arias et al. [25] for CO oxidation over CuO-CeO_2 catalysts. The mechanism assumes that copper and cerium cations on the catalyst are oscillating together between reduced and oxidized states during the reaction. The Cu^{2+} and Ce^{4+} are reduced by the reactant CO to Cu^+ and Ce^{3+} with formation of an oxygen vacancy on the catalyst. The reduced species are then reoxidized to their initial oxidation states by the oxygen in the reaction mixture. For the PROX reaction, Sedmak et al. extended the mechanism to both CO and H_2 oxidation over CeO-CeO_2 catalysts [15].

The redox mechanism assumes the presence of Cu^{2+} on CuO-CeO_2 during reaction and also the competition of CO and H_2 for the same catalytic sites, namely Cu^{2+}. Although Cu^{2+} has been shown to exist on the catalyst before the reaction or reductive treatments with CO or H_2, the presence of Cu^{2+} during or after the reaction has not been experimentally verified. On the contrary, according to X-ray photoelectron spectroscopy (XPS) spectra taken after the PROX reaction or reduction under H_2, only a mixture of Cu^+ and Cu^0 were found to stably coexist on CuO-CeO_2 [20,29]. If the amount of Cu^{2+} during the reaction is too small to be detected by XPS, then the mechanism should assign an extraordinarily high catalytic

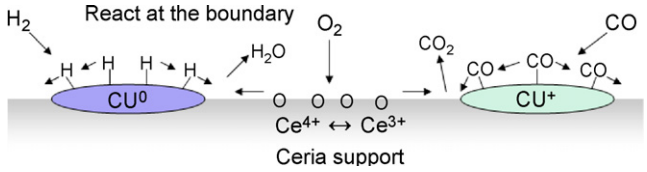

Fig. 10. Reaction model of CO and H_2 oxidation over CuO-CeO_2 catalyst in hydrogen mixtures.

activity to the Cu^{2+} species to explain the high performance of the catalyst in the PROX reaction. In view of the mild reaction conditions, this seems highly unlikely. Moreover, it is difficult to explain the independence of the CO and H_2 oxidation rates, observed under a variety of experimental conditions, if CO and H_2 compete with each other for adsorption on Cu^{2+}.

Liu and Flytzani-Stephanopoulos [14,19] compared the XPS spectra of a CuO-CeO_2 catalyst before and after a nitric acid treatment. The treatment was employed to remove the CuO in excess of the solid solution formed between copper and ceria in the catalyst. They observed the Cu^{2+} species on the catalyst by XPS, but the signal disappeared after the treatment and they could identify only Cu^+ species on the catalyst. In CO oxidation, however, the treated catalyst was as active as the untreated CuO-CeO_2 catalysts. Among their CuO-CeO_2 catalysts, the catalyst with 1 at% Cu content was absent of Cu^{2+} species even it was calcined in air at high temperatures, although Cu^+ was identified on the catalyst before and after the calcinations. Nevertheless, the catalyst with 1 at% Cu was similarly active in the CO oxidation with other catalysts. This shows that the stable Cu^+ was responsible for the activity and was not oxidized to Cu^{2+} by the oxidizing treatment. Clearly the redox between Cu^{2+} and Cu^+, postulated in the mechanism proposed by previous investigators [15,25], was not involved in the CO oxidation over the CuO-CeO_2 catalysts. An analysis of the redox processes under CO and O_2 indicated that the redox changes occur mainly in the ceria component, while the copper component is stabilized at the Cu^+ state [23,30].

Based on the discussion above, we propose a reaction model for the PROX reaction over the CuO-CeO_2 catalyst, as shown schematically in Fig. 10. In the model, CO and H_2 adsorb on Cu^+ and Cu^0 sites, respectively. The adsorbed species migrates to the interface between the copper components and the ceria support, where it reacts with the oxygen supplied by the ceria. During this, the cerium cation Ce^{4+} is reduced to Ce^{3+} and an oxygen vacancy is created. The molecular oxygen in the reaction mixture replenishes the vacancy and restores the oxidation state of the cerium cation to Ce^{4+}. For the CO oxidation, the proposed reaction model is similar to the model by Liu and Flytzani-Stephanopoulos [14].

5. Conclusion

The kinetics of CO oxidation and H_2 oxidation over a CuO-CeO_2 in H_2-rich mixtures containing CO_2 and H_2O have been investigated, and the power-law rate expressions, Eqs. (9) and (10), are presented for the CO oxidation and H_2 oxidation, respectively. The CO oxidation rate and H_2 oxidation rate are practically independent with each other and also independent of the O_2 partial pressure, as long as O_2 is available in the reaction mixture. Consequently, the CO oxidation rate is dependent on the partial pressures of CO, CO_2 and H_2O, while the H_2 oxidation rate is dependent on the partial pressures of H_2, CO_2 and H_2O. The CO_2 and H_2O in the reaction mixture inhibit both oxidations, and as a result, the oxidation rates have negative reaction orders with respect to the partial pressures of CO_2 and H_2O.

If CO and H_2 competed for the same active site to adsorb, the CO oxidation rate must have shown a certain dependency on the H_2 partial pressure and also the H_2 oxidation rate on the CO partial pressure. The independence between the two oxidation rates indicates that the adsorption sites for CO and H_2 are necessarily different. In view of this and literature results, we propose a reaction model, in which CO selectively adsorbs on the Cu^+ species and H_2 dissociates on the Cu^0 species; the adsorbed species migrates to the interface between the copper components and the ceria support, and reacts with the oxygen provided by the ceria support; and the oxygen in the reaction mixture replenishes the oxygen deficiency on the support.

Acknowledgement

The Korea Gas Corporation is gratefully acknowledged for financial support.

References

[1] D.H. Kim, M.S. Lim, Appl. Catal. A 224 (2002) 27.
[2] M.J. Kahlich, H.A. Steiger, R.J. Behm, J. Catal. 171 (1997) 93.
[3] A. Manaslip, E. Gulari, Appl. Catal. B: Environ. 37 (2002) 17.
[4] E.J. Bissett, S.H. Oh, Chem. Eng. Sci. 60 (2005) 4722.
[5] C.D. Dudfield, R. Chen, P.L. Adcock, Int. J. Hydrogen Energy 26 (2001) 763.
[6] O. Kotrotkikh, R. Farrauto, Catal. Today 62 (2000) 249.
[7] G. Avgouropoulos, T. Ioannides, H.K. Matralis, J. Batista, S. Hovevar, Catal. Lett. 73 (2001) 33.
[8] G. Avgouropoulos, T. Ioannides, Ch. Papadopoulos, J. Batista, S. Hovevar, H.K. Matralis, Catal. Today 75 (2002) 157.
[9] G. Avgouropoulos, T. Ioannides, Appl. Catal. A 244 (2003) 155.
[10] D.H. Kim, J.E. Cha, Catal. Lett. 86 (2003) 107.
[11] C.M. Bae, J.B. Ko, D.H. Kim, Catal. Commun. 6 (2005) 507.
[12] F. Marino, C. Descorme, D. Duprez, Appl. Catal. B: Environ. 58 (2005) 175.
[13] Y.Z. Chen, B.J. Liaw, H.C. Chen, Int. J. Hydrogen Energy 31 (2006) 427.
[14] W. Liu, M. Flytzani-Stephanopolous, J. Catal. 153 (1995) 317.
[15] G. Sedmak, S. Hocevar, J. Levec, J. Catal. 213 (2003) 135.
[16] G. Sedmak, S. Hocevar, J. Levec, J. Catal. 222 (2004) 87.
[17] C. Descorme, R. Taha, N. Mouaddib-Moralb, D. Duprez, Appl. Catal. A 223 (2002) 287.
[18] J.L. Kuester, J.H. Mize, Optimization Techniques with Fortran, McGraw-Hill, New York, 1973, pp. 298.
[19] W. Liu, M. Flytzani-Stephanopolous, J. Catal. 153 (1995) 304.
[20] H. Zou, X. Dong, W. Lin, Appl. Surf. Sci. 253 (2006) 2893.
[21] J. Wang, S.-C. Lin, T.-J. Huang, Appl. Catal. A 232 (2002) 107.
[22] X. Tang, B. Zhang, Y. Li, Y. Xu, Q. Xin, W. Shen, Appl. Catal. A 288 (2005) 116.
[23] A. Martinez-Arias, A.B. Hungria, M. Fernandez-Garcia, J.C. Conesa, G. Munuera, J. Phys. Chem. B 108 (2004) 17983.
[24] A. Dandekar, M.A. Vannice, J. Catal. 178 (1998) 621.

[25] A. Martinez-Arias, M. Fernandez-Garcia, O. Galvez, J.M. Coronado, J.A. Anderson, J.C. Conesa, J. Soria, G. Munuera, J. Catal. 195 (2000) 207.
[26] A. Martinez-Arias, A.B. Hungria, G. Munuera, D. Gamarra, Appl. Catal. B 65 (2006) 207.
[27] D. Gamarra, A. Hornés, Zs. Koppány, Z. Schay, G. Munuera, J. Soria, A. Martínez-Arias, J. Power Sources 169 (2007) 110.
[28] M.J.L. Gimes, A.J. Marchi, C.R. Apesteguia, Appl. Catal. A 154 (1997) 155.
[29] C. Lamonier, A. Ponchel, A. D'Huysser, L. Jalowiecki-Duhamel, Catal. Today 50 (1999) 247.
[30] A. Martinez-Arias, D. Gamarra, M. Fernandez-Garcia, X.Q. Wang, J.C. Hanson, J.A. Rodriguez, J. Catal. 240 (2006) 1.